Pergamon

Bioorganic & Medicinal Chemistry 6 (1998) 2085–2101

BIOORGANIC & MEDICINAL CHEMISTRY

Binding of Peptides in Solution by the *Escherichia coli* Chaperone PapD as Revealed Using an Inhibition ELISA and NMR Spectroscopy

Katarina Flemmer Karlsson,[a] Björn Walse,[b] Torbjörn Drakenberg,[b] Sarbari Roy,[a] Karl-Erik Bergquist,[a] Jerome S. Pinkner,[c] Scott J. Hultgren[c] and Jan Kihlberg[d,*]

[a]*Organic Chemistry 2, Center for Chemistry and Chemical Engineering, Lund University, PO Box 124, S-221 00, Lund, Sweden*
[b]*Physical Chemistry 2, Center for Chemistry and Chemical Engineering, Lund University, PO Box 124, S-221 00, Lund, Sweden*
[c]*Department of Molecular Microbiology, Washington University School of Medicine, Box 8230, St. Louis, MO 63110-1093, USA*
[d]*Organic Chemistry, Umeå University, S-901 87 Umeå, Sweden*

Received 23 March 1998; accepted 18 June 1998

Abstract—PapD is the prototype member of a family of periplasmic chaperones which are required for assembly of virulence associated pili in pathogenic, gram-negative bacteria. In the present investigation, an ELISA has been developed for evaluation of compounds as inhibitors of PapD. Synthetic peptides, including an octamer, derived from the C-terminus of the pilus adhesin PapG were able to inhibit PapD in the ELISA. Evaluation of a panel of octapeptides in the ELISA, in combination with NMR studies, showed that the peptides were bound as extended β-strands by PapD in aqueous solution. The PapD–peptide complex was stabilized by backbone to backbone hydrogen bonds and interactions involving three hydrophobic peptide side chains. This structural information, together with previous crystal structure data, provides a starting point in efforts to design and synthesize compounds which bind to chaperones and interfere with pilus assembly in pathogenic bacteria.

Introduction

Many gram-negative bacteria assemble extracellular adhesive organelles termed pili on their surfaces that allow them to colonize host tissue and give rise to infections.[1] This group of bacteria includes pathogens that cause a variety of diseases, such as urinary tract infection and the more severe pyelonephritis, meningitis, whooping cough, pneumonia and diarrhoea.[2] Pili are rodlike, supramolecular protein fibers that present adhesins at their tip for specific attachment to receptors found in the host.[3,4] The P pilus of uropathogenic *Escherichia coli* is the best characterized of all bacterial pili and carries the adhesin PapG at the end of a thin tip fibrillum joined to a thicker pilus rod.[1] The mode of binding of the PapG adhesin to the receptor-active disaccharide, α-D-galactopyranosyl-(1-4)-β-D-galactopyranose [Galα(1-4)Galβ], present in the globoseries of glycolipids on kidney epithelium cells,[5,6] has been revealed in detail using synthetic receptor analogues.[7–9] The P pilus tip fibrillar structure is composed of repeating PapE subunits whereas the pilus rod consists of large numbers of the major pilin subunit PapA. The adaptor proteins PapF, PapK, and PapH join the different parts of the pilus to each other and anchor the pilus in the outer cell membrane of the bacteria. All bacterial pilus assembly requires the presence of periplasmic chaperones. P pili are assembled by the chaperone PapD that binds to and caps interactive surfaces on each pilus subunit thus preventing premature aggregation during their secretion into the periplasmic space.[10–12] The crystal structure of PapD has been solved at 2.5 Å resolution and reveals that PapD consists of two β-barrel domains oriented in

Key words: Pili; chaperone; ELISA; peptide; structure–activity; NMR spectroscopy.
*Corresponding author. Tel.: 46 90 786 6890; fax: 46 90 13 88 85; e-mail: jan.kihlberg@chem.umu.se

0968-0896/98/$ - see front matter
PII: S0968-0896(98)00162-X

the shape of a boomerang.[13] Furthermore, PapD has been found to have significant sequence homology (25–56% identity) with chaperones that assemble other types of pili suggesting that all chaperones have closely related structures.[2,14]

The C-terminus of the P pilus proteins has been indicated to constitute an essential part of the epitope on each subunit that is recognized by the PapD chaperone.[10,12,15,16] Thus, truncation of the C-terminal 13 residues in the adhesin PapG abolished complex formation with PapD.[10] Moreover, synthetic 19-mer peptides from the C-terminus of P-pilus proteins bound to PapD and some of these peptides also inhibited chaperone mediated folding of the adhesin PapG in an in vitro assay.[15] The crystal structure of PapD bound to the C-terminal 19-mer peptide from PapG (PapG296-314), determined at 3.0 Å resolution, suggested a structural basis for chaperone-subunit interactions.[15] It was found that the peptide was anchored by hydrogen and ionic bonding of the C-terminal carboxylate group to residues Arg^{8} and Lys^{112}, which are found in the cleft of PapD and are invariant in the chaperone superfamily. Seven main-chain hydrogen bonds were also formed between the peptide backbone and the G1 β-strand on the surface of PapD resulting in a parallel β-strand interaction. Furthermore, the hydrophobic side chains of Phe^{313}, Leu^{311}, Met^{309}, and Met^{307} in the peptide made significant contact with PapD. Interestingly, these hydrophobic residues are part of a conserved pattern of alternating hydrophobic and hydrophilic residues present in the C-terminus of pilus proteins.[15] However, within the crystal, the PapD-peptide β-sheet was extended even further, since a second PapD-peptide complex was placed adjacent to the first, so that the two bound peptide chains interacted as antiparallel β-strands. It can not be ruled out that the structure of the complex was significantly influenced by this dimerization.

In addition to providing information on how chaperones recognize pilus proteins, studies of the interactions between synthetic peptides and chaperones provide structural information that may be used for design and synthesis of ligands that bind to chaperones. By inhibiting pilus assembly, such compounds would interfere with bacterial attachment to the host; therefore, they constitute potential novel antibiotics. It was recently pointed out that the development of compounds that interfere with bacterial protein secretion (for instance, in pilus assembly) constitutes an attractive approach to overcome widespread bacterial resistance to existing antibiotics.[17] However, such efforts have been hampered by the lack of bioassays, which properly evaluate compounds as inhibitors of the critical complex formation between chaperone and pilus protein.[15] Therefore, we have developed an enzyme-linked immunosorbent assay (ELISA) in which compounds may be evaluated for their ability to inhibit complex formation between PapD and a fusion protein (MaltBP–PapG175-314)[16] which consists of the chaperone binding domain of the PapG linked to the maltose binding protein. Evaluation of a panel of synthetic peptides derived from the C-terminus of P pilus proteins in the assay resulted in the identification of a minimal inhibitory octapeptide. Investigation of alanine and serine scans of this octapeptide in the ELISA, in combination with NMR studies of two peptide–PapD complexes, revealed structural details responsible for the formation of complexes between PapD and peptides in aqueous solution.

Results

Synthesis of pilus-related peptides and a reduced analogue

To enable the present investigation, a number of peptides derived from the C-terminus of the proteins which make up the P pilus have been prepared (peptides are denoted by their pilus protein origin and the fragment they represent within this protein; sequences are shown in Table 1). These synthetic peptides include the five 19-mer peptides (PapG296-314, PapF130-148, PapE131-149, PapK139-157, and PapH155-173)[18] as well as the length series from PapG (ranging in length from C-terminal 19- to 6-mer) and PapH (C-terminal 22- to 8-mer). The C-terminal octamer peptides from the six pilus subunits, alanine- and serine-scan series of the octapeptide PapG307-314, and several controls have also been prepared. All peptides were prepared on solid phase according to the Fmoc strategy using a fully automatic peptide synthesizer[19] constructed in our laboratory. As reported previously, use of a polystyrene resin grafted with polyethylene-glycol spacers (TentaGel PEG PS resin) was important for the successful preparation of the 19-mer pilus subunit derived peptides.[18] After TFA-catalyzed cleavage from the solid phase, the peptides were purified to greater than 95% homogeneity by reversed-phase HPLC and their structures were confirmed by NMR spectroscopy (selected peptides only) and mass spectrometry. Peptides corresponding to sequences located internally in pilus proteins (i.e. PapG299-306, PapG296-313, PapG306-313, and PapH155-165) were prepared as C-terminal amides; whereas all other peptides had a free C-terminal carboxyl group. The N-terminal amino group of the peptides was kept free in all cases, in order to improve solubility.

The peptide PapG307-314*red* (**8**), in which the α-carboxyl group of Pro^{314} has been reduced (Scheme 1), was prepared in order to probe the importance of the C-terminal carboxyl group for anchoring to PapD.

Table 1. Amino acid sequences for the C-terminus of the proteins PapG, F, E, K, A, and H that are assembled into the *E. coli* P pilus

	Position from C-terminus																		
Peptide[a]	19	18	17	16	15	14	13	12	11	10	9	8	7	6	5	4	3	2	1
PapG296-314	G	K	R	K	P	G	E	L	S	G	S	M	T	M	V	L	S	F	P
PapF130-148	G	I	L	N	G	G	D	F	Q	T	T	A	S	M	S	M	I	Y	N
PapE131-149	Q	N	L	I	A	G	P	F	S	A	T	A	T	L	V	A	S	Y	S
PapK139-157	K	S	V	V	P	G	D	Y	E	A	T	A	T	F	E	L	T	Y	R
PapA145-163[b]	A	A	V	T	E	G	A	F	S	A	V	A	N	F	N	L	T	Y	Q
PapH155-173	K	K	L	E	A	G	N	Y	F	A	V	L	G	F	R	V	D	Y	E
Residue type[c]			H[d]			C[e]		H[d]	P[f]				P[f]	H[d]		H[d]	P[f]	H[d]	P[f]

[a] The residues in the peptides are numbered as in the corresponding pilus subunits, which lack the signal sequence.
[b] Synthetic peptide not available due to difficulties in purification.
[c] Only positions where at least five out of six residues belong to the same type have been included.
[d] H = Hydrophobic aromatic or aliphatic residue.
[e] C = Conserved glycine.
[f] P = Polar or charge residue.

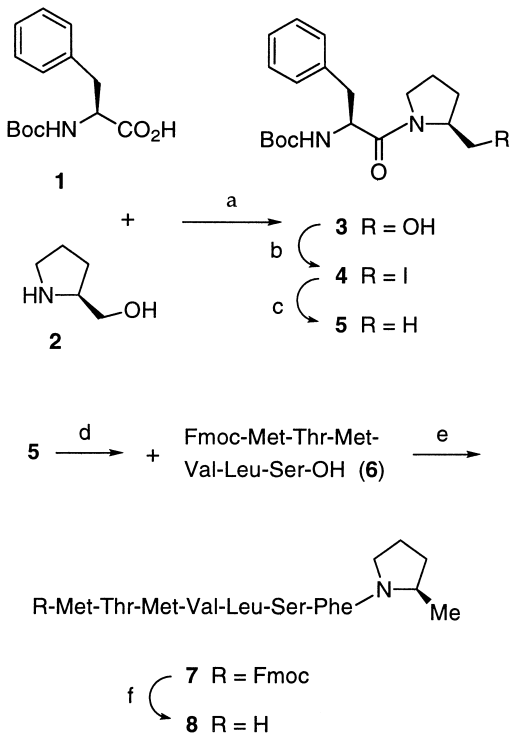

Scheme 1. (a) TBTU, *N*-methylmorpholine, DMF (77%); (b) I_2, Ph_3P, imidazole, toluene, 80 °C (64%); (c) H_2, Pd/C, Et_3N, EtOAc:EtOH 1:5 (93%); (d) HCl, HOAc; (e) HATU, HOAt, trimethylpyridine, DMF, 0 °C→rt (53%); (f) 20% piperidine in DMF (~26%).

Synthesis of **8** was achieved by coupling of the reduced Phe-Pro analogue **5** with hexapeptide fragment **6**. The dipeptide **5** was prepared by condensation of N^{α}-*tert*-butoxycarbonyl (Boc) protected phenylalanine (**1**) with prolinol (**2**), promoted by *O*-(benzotriazol-1-yl)-1,1,3,3-tetramethyluronium tetrafluoroborate (TBTU), to give **3**. Substitution of the hydroxyl group in **3** was accomplished by treatment with iodine, triphenylphosphine, and imidazole[20] to give the iodide **4**, which on catalytic hydrogenation gave **5**. Substantial *cis*/*trans* isomerism (20–40% *cis*) was observed for the amide bond in compounds **3–5**, as revealed by the characteristic $d_{\alpha\delta}(i,i+1)$ NOE observed between Phe-Hα and Pro-Hδ for the *trans*-form and the $d_{\alpha\alpha}(i,i+1)$ NOE between the Phe and Pro Hα protons of the *cis*-form. After cleavage of the Boc-protective group, reduced dipeptide **5** was coupled with Fmoc-protected fragment **6** using the highly active coupling reagent, *O*-(7-azabenzotriazol-1-yl)-1,1,3,3-tetramethyluronium hexafluorophosphate (HATU)[21] in combination with 1-hydroxy-7-azabenzotriazole (HOAt)[22] and collidine to give **7**. Collidine has been recommended for use in peptide-fragment coupling reactions to avoid racemization of the activated, C-terminal amino acid.[23] Finally, cleavage of the Fmoc group in **7** by treatment with piperidine gave **8**.

Peptides as inhibitors of complex formation between PapD and the PapG adhesin

The PapD–MaltBP–PapG175-314 inhibition ELISA. In order to allow investigations of the ability of various compounds, such as peptides derived from the subunits of the *E. coli* P pilus, to inhibit complex formation between the PapD chaperone and pilus proteins, an enzyme-linked immunosorbent assay (ELISA) was developed. This ELISA was based on the MaltBP–PapG175-314 fusion protein[16] that consists of the 140 C-terminal amino acids of the PapG adhesin linked to the maltose binding protein. In contrast to PapG itself, the MaltBP–PapG175-314 fusion protein can be purified

in native form in the absence of PapD. Furthermore, the complex between PapD and MaltBP–PapG175-314 has been shown to be as stable as the native PapD–PapG complex,[16] which is the most stable of the complexes formed between PapD and the proteins that make up the P pilus. This argues that the ELISA is a relevant model for studies of ligands that bind to the PapD chaperone.

In the inhibition ELISA microtiter-plate-wells were coated with the MaltBP–PapG175-314 fusion protein and then blocked with BSA. Peptides to be investigated as inhibitors were dissolved in DMSO and preincubated with the PapD chaperone in PBS (DMSO was required as a cosolvent due to the low solubility of most of the peptides in aqueous solutions). The coated and blocked microtiter-plate-wells were then incubated with the peptide–PapD solution. PapD bound to MaltBP–PapG175-314 in the wells was detected by addition of anti-chaperone antibody (rabbit IgG) followed by goat antiserum to rabbit IgG conjugated to alkaline phosphatase. As compared to a preliminary report[24] describing the inhibition ELISA, all incubation times and the protein-stabilizing agent used during incubation of the coated wells with peptide–PapD solution were optimized. This resulted in lower background readings as well as higher and substantially more reproducible levels of inhibition for the peptides.

Peptides from the C-terminus of the adhesin PapG and the membrane anchor PapH inhibit complexation of PapD to PapG

The C-terminal 19-mer peptides from the pilus adhesin PapG and the membrane anchor protein PapH (PapG296-314 and PapH155-173, cf. Table 1 for sequences) were both potent inhibitors of complex formation between PapD and MaltBP–PapG175-314 (Fig. 1A). The inhibitory power of PapG296-314 reached a maximum at a peptide/PapD ratio of ~100 and inhibition then decreased as the ratio was increased. This reduction in inhibitory power was assumed to be due to limited solubility of PapG296-314 under the conditions of the ELISA, aggregation of the peptide or peptide–PapD complex, or combinations of these phenomena. The 19-mer peptides PapE131-149 and PapK139-157, which are derived from proteins that make up the flexible pilus tip, did not show any significant inhibitory power. PapF130–148, also derived from a pilus tip protein, gave highly irreproducible results in the ELISA and often induced increased binding of PapD to MaltBP–PapG175-314 (data not shown). The effect was tentatively explained as originating from formation of peptide aggregates that promote complexation of PapD and MaltBP–PapG175-314. The 19-mer peptide from the C-terminus of PapA, the subunit making

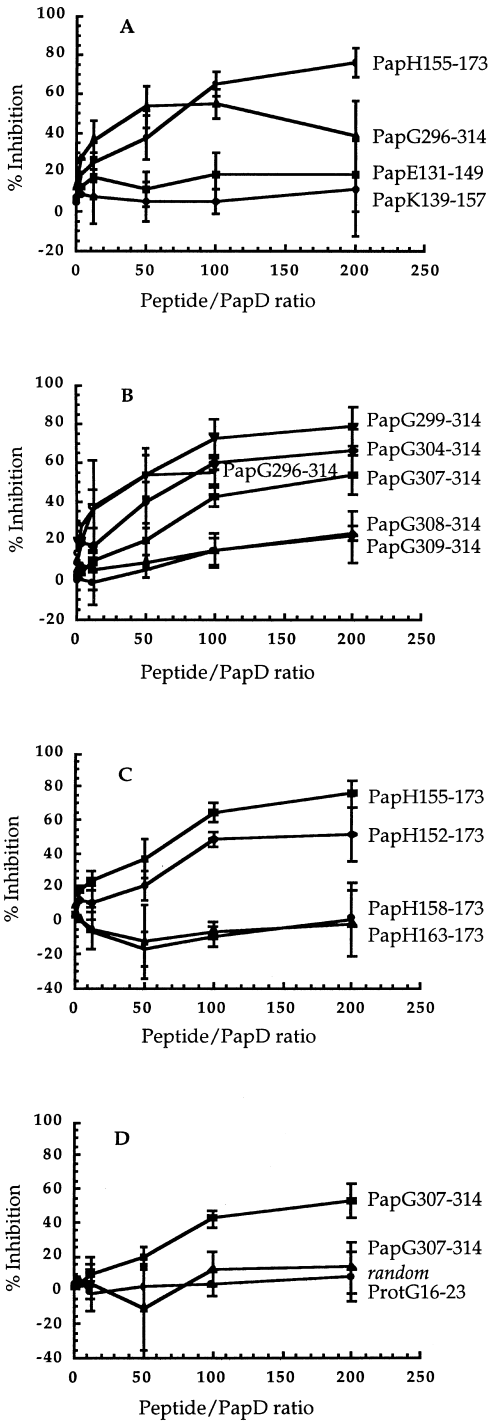

Figure 1. Inhibition of binding of PapD to the MaltBP–PapG175-314 fusion protein using (A) 19-mer peptides from the C-terminus of P pilus proteins, (B) a length series of peptides derived from the C-terminus of the pilus adhesin PapG, (C) a length series of peptides derived from the C-terminus of the pilus anchor PapH and (D) the octapeptide PapG307-314 and two peptide controls (error bars represent 95% confidence limits).

up the bulk of the pilus rod, could not be satisfactorily purified after synthesis and was therefore not available for investigation in the ELISA.

The minimum length of peptides from PapG and PapH required for inhibition of binding of PapD to MaltBP–PapG175-314 was investigated using two length series of peptides, all members of which had the C-terminal residue in the pilus protein as their last residue. The PapG series consisted of the 19-, 16-, 11-, 8-, 7-, and a 6-mer; whereas, the PapH series included the 22-, 19-, 16-, 11-, and 8-mer. In the PapG series, the inhibitory power increased successively as the peptide length increased (Fig. 1B). Interestingly, the octapeptide PapG307-314 was significantly more potent than the heptapeptide PapG308-314; whereas, the differences in inhibitory power between the octapeptide and PapG304-314 (11-mer) and between the 11-mer and PapG299-314 (16-mer) were minor and not significant. However, the inhibitory power of the 16-mer PapG299-314 was significantly higher than that of octapeptide PapG307-314. The peptide PapG299-306, representing an internal PapG sequence, was not able to inhibit complex formation between PapD and MaltBP–PapG175-314 (data not shown). Altogether, these results show that octa-undecamer peptides derived from the very C-terminus of PapG contain the essential structural features required for binding to PapD and inhibition of complex formation with the PapG adhesin. In the PapH series, only the 19-mer PapH155-173, and the even longer 22-mer PapH152-173, were able to inhibit complex formation between PapD and MaltBP–PapG175-314 (Fig. 1C). The shorter 8-mer (PapH166-173), 11-mer (PapH163-173), and 16-mer (PapH158-173), as well as the 11-mer PapH155-165 that represents an internal PapH sequence (data not shown), were all devoid of activity. Thus, in contrast to the octamer binding motif in PapG, at least the 17 C-terminal amino acid residues in PapH are required for inhibition of binding of PapD to PapG.

The octamer C-terminal peptides from the remaining four pilus subunits (PapF, PapE, PapK, and PapA) were also analyzed for inhibitory activity in the ELISA. However, with the possible exception of PapK150-157, these peptides were not able to significantly inhibit complex formation between PapD and MaltBP–PapG175-314 (data not shown). The lack of inhibitory power displayed by the five C-terminal octamer peptides from the pilus proteins PapF, E, K, A, and H, as compared to the corresponding octamer from PapG, indicates the importance of specific interactions between peptide side chains and PapD. This was further investigated using the peptides PapG307-314*random* (Leu-Met-Ser-Phe-Val-Met-Thr-Pro), which contains the same amino acids as PapG307-314, but incorporated in a different order, and ProtG16-23 (Thr-Leu-Lys-Gly-Glu-Thr-Thr-Thr), derived from a part of protein G that interacts as an antiparallel β-strand with immunoglobulin F_{ab} fragments.[25] Both these peptides lacked inhibitory power (Figure 1D), further confirming that the side chains of peptides from PapG, in addition to hydrogen bonds from the peptide backbone, form important contacts with the PapD chaperone.

Three hydrophobic side chains in the C-terminal octamer peptide from PapG (PapG307-314) are important for binding to PapD

The role of the side chains of the minimal inhibitory peptide from PapG (PapG307-314) in binding to PapD was investigated using an alanine and a serine scan series of peptides. In the alanine scan series all residues of PapG307-314 were replaced, one by one, by alanine, whereas Ser^{312} and Thr^{308} were excluded in the analogous serine scan series. Comparison of the inhibitory power of the alanine and serine mutant at each position in PapG307-314, with that of native PapG307-314, revealed the role of that particular side chain for binding to PapD (Fig. 2). Some of the peptides containing Ala mutations displayed a low solubility and/or a tendency to aggregate which had to be taken into account on evaluation of their inhibitory power. The Ser mutants of PapG307-314 did not suffer from such problems and results obtained with this peptide series were therefore more readily interpreted.

The residues with even numbers in PapG307-314, i.e. those not in contact with PapD in the crystalline complex, do not appear to be important for binding to PapD. Replacement of Pro^{314} with Ala or Ser did not reduce the inhibitory power of PapG307-314 (Fig. 2A). This was also found on substitution of Ser^{312} by Ala (Fig. 2C). For Val^{310}, the Ser mutant is equally potent as the native peptide; whereas, the Ala mutant appears to be inhibitory at low peptide/PapD ratios, but not at higher ratios (Fig. 2E). As discussed for the 19-mer PapG296-314, the decrease in inhibitory power of the Val^{310}→Ala substitution in PapG307-314 with increasing concentration most likely originates from low solubility and/or aggregation of the peptide in the ELISA, rather than from a low intrinsic activity. The role of Thr^{308} is less clear since the alanine mutant peptide promotes binding of PapD and MaltBP–PapG175-314 (Fig. 2G). A similar behavior was observed for the 19-mer PapF130-148 and was tentatively assumed to result from limited solubility or aggregation of the peptide.

In contrast, three of the residues with odd numbers in PapG307-314, which contact PapD in the crystalline complex, were found to be important for interaction

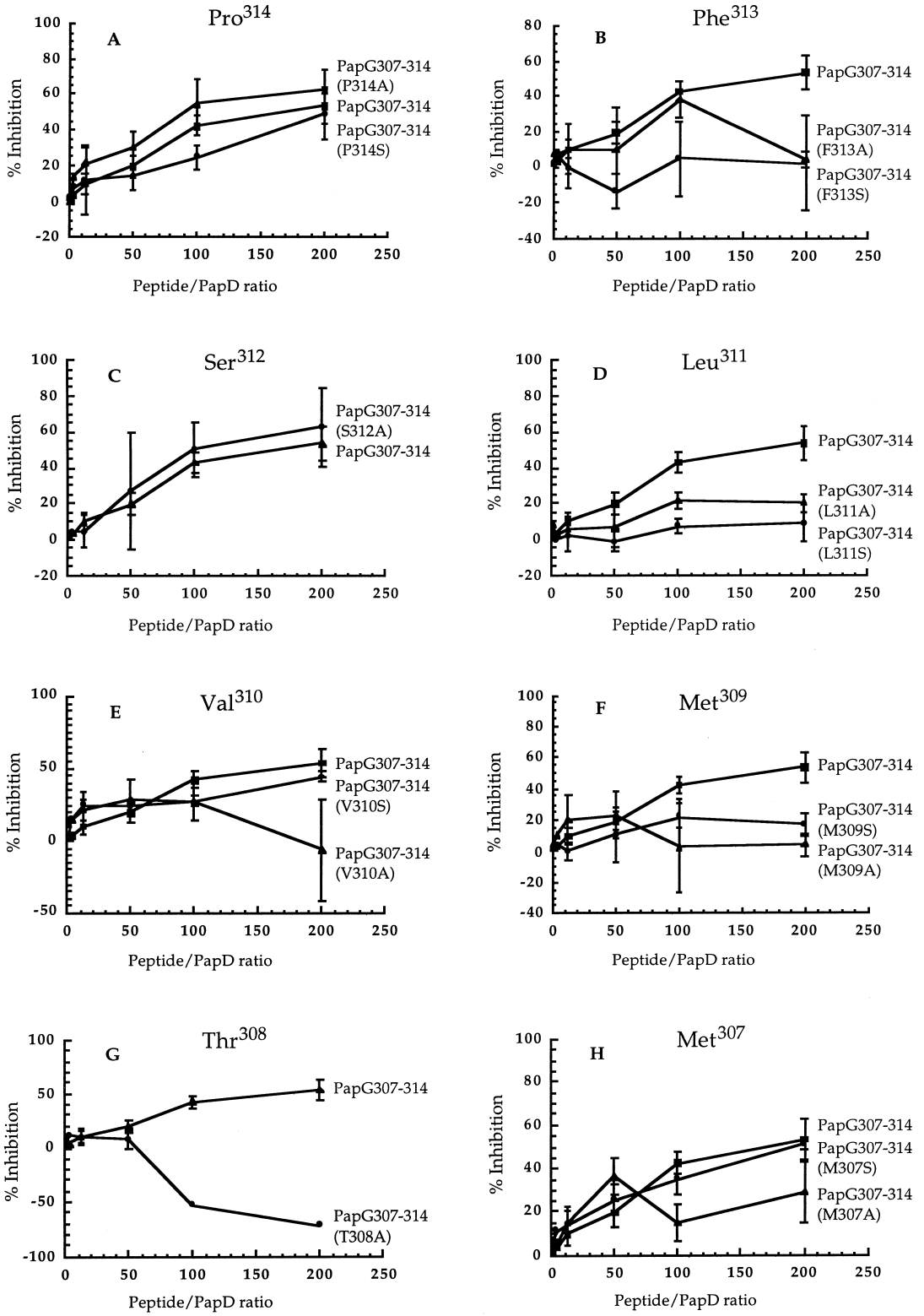

Figure 2. Inhibition of binding of PapD to the MaltBP–PapG175-314 fusion protein using an alanine and a serine scan series of the octapeptide PapG307-314 (error bars represent 95% confidence limits).

with PapD. Replacement of Phe^{313} by Ala did not lead to a reduction in inhibitory power, because the drop in inhibition at the highest peptide/PapD ratio was again considered to result from low solubility and/or aggregation (Fig. 2B). However, replacement of Phe^{313} by Ser abolished the peptides inhibitory power, signaling that Phe^{313} is involved in a weak hydrophobic interaction with PapD. This conclusion was further supported by the observation that substitution of Phe^{313} for Tyr led to a reduction in inhibitory power (data not shown). For Leu^{311} and Met^{309}, both the Ala and Ser mutants were, at best, weak inhibitors revealing the importance of these residues for binding to PapD (Fig. 2D and F). Met^{307} does not appear to be essential for binding to PapD since the Ser mutant is equally potent as native PapG307-314, whereas the irregular behavior of the Ala mutant presumably reflects low solubility or a tendency to aggregate (Fig. 2H).

Anchoring of the C-terminal carboxyl group of peptides to invariant residues in PapD is not critical

The importance of 'anchoring' the C-terminal carboxyl group of an inhibitory peptide to Arg^8 and Lys^{112} in the binding site of PapD by hydrogen bonding and by a salt bridge was probed in two different ways. The peptide PapG307-314*red* (cf. **8**, Scheme 1), in which the C-terminal carboxyl group has been reduced to a methyl group, was found to be a slightly less powerful inhibitor of complex formation between PapD and MaltBP–PapG175-314 than PapG307-314 (Fig. 3). This suggests only a minor role for anchoring to Arg^8 and Lys^{112} in peptide–PapD complexes. This conclusion was further supported using the peptide PapG306-313, which lacks Pro^{314}, and was at least as powerful an inhibitor as the native octamer PapG307-314. In view of the importance of the side chains Phe^{313}, Leu^{311}, and Met^{309} for interaction with PapD, it was assumed that PapG306-313 binds to PapD with these three residues in their respective binding sites on the chaperone. Consequently, interactions between the peptide C-terminus and Arg^8 and Lys^{112} in PapD are not possible.

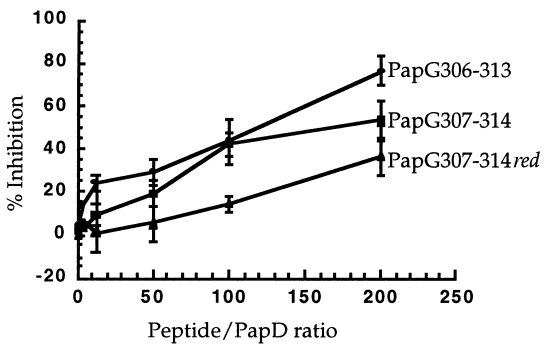

Figure 3. Inhibition of binding PapD to the MaltBP–PapG175-314 fusion protein using peptides from the adhesin PapG which lack the C-terminal Pro^{314} (PapG306-313) or in which the C-terminal carboxyl group has been reduced to a methyl group (PapG307-314*red*) (error bars represent 95% confidence limits).

^{1}H NMR studies of 19-mer peptides from the C-terminus of pilus proteins

^{1}H NMR studies were undertaken to investigate if different conformational preferences between the 19-mer peptides PapG296-314, PapE131-149, PapK139-157, and PapH155-173 could explain the differences in their inhibitory power. The latter three peptides were insoluble in aqueous solution at a pH close to 6 and the NMR studies were therefore carried out in DMSO at 27 °C. DMSO was chosen since all peptides employed in the present investigation were evaluated in the ELISA in mixtures of water and DMSO, where the DMSO content ranged from 1 to 50%. However, it should be pointed out that the conformational preferences in DMSO might be different from those in aqueous DMSO, making conclusions only tentatively valid under the conditions used in the ELISA. In DMSO, sequence-specific assignments of the residues in the peptides were obtained based on COSY, TOCSY, ROESY, and NOESY spectra according to standard procedures.[26] Two sets of resonances were observed in the NMR spectra of PapG296-314 and PapE131-149, which originated from *cis*/*trans* isomerism about the amide bond between Phe^{313} and Pro^{314} in PapG296-314 and between Gly^{136} and Pro^{137} in PapE131-149, respectively. The major *trans* forms displayed the characteristic NOEs between Pro Hδ and Hα of the preceding residue, whereas the minor *cis* forms displayed the equally characteristic NOEs between Pro Hδ and Hα of the preceding residue. Integration in the one-dimensional ^{1}H NMR spectra showed the *cis* content to be ~20% for PapG296-314 and 25–30% for PapE131-149. PapG296-314 also contains a proline at position 300, whereas PapK139-157 has a proline at position 143. The amide bonds to both of these prolines existed predominantly in the *trans* form.

Strong or medium intensity $H\alpha_i/NH_{i+1}$ NOE connectivities, as well as medium intensity NH_i/NH_{i+1} NOEs, were observed along most or all of the peptide chains of the four peptides. No medium or long range NOEs could be detected. Since β-strands display strong $H\alpha_i/NH_{i+1}$ NOEs and lack NH_i/NH_{i+1} NOEs, whereas the opposite is found for α-helices, these NOEs indicate that the four 19-mer peptides are conformationally averaged between both the α_R and the β region of the ϕ,Ψ-space.[26,27] When compared to random-coil chemical shift values determined for model peptides,[28] the Hα protons in the four 19-mer peptides were shifted slightly upfield (less than 0.15 ppm), except for Lys^{299} and

Phe^{313} in PapG296-314 and Gly^{136} in PapE131-149 which display downfield shifts. The latter observation may, however, well be explained by the observation that proline has been found to induce a ~0.3 ppm downfield shift for the preceding residue.[29] Thus, both NOEs and Hα chemical shifts indicate that the four peptides are conformationally averaged between the α_R and the β region of the φ,Ψ-space in DMSO. This conclusion was also reached in a previous study of the conformation of PapG296-314 in aqueous solution using ^{1}H NMR spectroscopy.[18]

NMR studies of complexes between PapD and peptides from PapG

The complexes between PapD and the C-terminal octa- and heptapeptide from the pilus adhesin PapG (PapG307-314 and PapG308-314, respectively) were studied by two different NMR techniques. Isotope-edited NMR spectroscopy[30] was used to study the complex between PapD and PapG307-314, in which all residues except Pro^{314} were ^{15}N-labeled. Unfortunately, the low solubility of PapG307-314 in aqueous solution at pH 6.0 did not allow studies of the unbound form of the octapeptide. However, on addition of PapD the peptide was dissolved thereby allowing investigation of its structure when bound by PapD. The heptapeptide PapG308-314 was more soluble in aqueous solution but did not bind to PapD with sufficient strength to permit studies of the complex using ^{15}N-edited NMR spectroscopy. Instead, the weak complex between PapG308-314 and PapD was studied by transferred nuclear Overhauser effect spectroscopy (TRNOE),[31] which requires a fast exchange of the ligand between the bound and free states thereby allowing NOEs developed for the ligand in the bound form to be detected in the free form.[32] In contrast to the NMR studies of the 19-mer peptides, DMSO was not used as solvent in these studies of PapG307-314 and PapG308-314.

Assignment of all the proton resonances in the free form of heptapeptide PapG308-314 was obtained from ROESY and TOCSY spectra (Table 2). Two forms of the peptide were observed, originating from *cis–trans* isomerization of the amide bond between Phe^{313} and Pro^{314}. The major form had a *trans* peptide bond and integration of the cross peaks for Pro^{314} in the TOCSY spectrum showed a *cis*-content of 40%. A similar *cis–trans* ratio has also been observed for the longer 19-mer PapG296-314 in aqueous solution.[18] Strong-intensity sequential $H\alpha_i/NH_{i+1}$ NOE connectivities were observed along the whole peptide chain but no sequential NH_i/NH_{i+1} NOEs or medium- or long-range NOEs could be detected. Only small deviations from the Hα proton chemical shifts of short random-coil peptides[29] were found for PapG308-314. Altogether, these observations indicate that the backbone dihedral angles of the PapG308-314 are averaged, but predominantly in the β (extended chain) region of φ,Ψ-space.[26,27]

In the complex between PapD and ^{15}N-labeled PapG307-314, sequential $H\alpha_i/NH_{i+1}$ NOE connectivities were observed for the sequence from Met^{309} to Phe^{313}. Taken together with the absence of both intraresidue $H\alpha_i/NH_i$ and sequential NH_i/NH_{i+1} NOEs this suggested that the peptide was bound to PapD in an extended β-strand conformation. This conclusion was further confirmed by the transferred NOEs obtained for the complex between PapD and PapG308-314. The NOESY spectrum of unbound PapG308-314 contains

Table 2. ^{1}H NMR chemical shifts (δ, ppm) for PapG308-314 in aqueous phosphate buffer (pH 6.0) containing 10% D_2O, obtained at 600 MHz and 27 °C. When determined, chemical shifts for the *cis* form about the Phe-Pro amide bond are given on the second row for a residue. Numbers in parentheses indicate the chemical shifts when PapD is present

Residue	NH	Hα	Hβ	Hγ	Others
Thr^{308}	[a]	4.09	3.81	1.26	
Met^{309}	[a]	4.53	1.98, 2.04 (2.01[b])	2.53[b]	2.08 (SMe)
Val^{310}	8.32	4.04 (4.05)	1.97	0.85, 0.90	
	8.33	4.07	2.00	0.90[b]	
Leu^{311}	8.32 (8.34)	4.33 (4.34)	1.43 (1.44), 1.56	1.56	0.83 and 0.90 (Hδ,δ′)
	8.37 (8.38)	4.40	1.54, 1.61	1.61	0.86 and 0.92 (Hδ,δ′)
Ser^{312}	7.99 (8.00[c])	4.36 (4.37[c])	3.66[b]		
	8.18	4.43	3.76[b]		
Phe^{313}	8.19	4.88	2.85, 3.20 (2.86, 3.21)		7.28 and 7.33 (H-arom)
	8.01	4.65	2.93[b]		7.23, 7.35, 7.31 (H-arom)
Pro^{314}		4.24 (4.25)	1.91, 2.20	1.97[b]	3.66 (3.67) and 3.71 (Hδ)
		3.66	1.80, 1.85	1.67[b]	3.30 and 3.47 (Hδ)

[a] Not observed due to fast amide proton exchange.
[b] Degeneracy has been assumed.
[c] Broad resonance, chemical shift determination is uncertain.

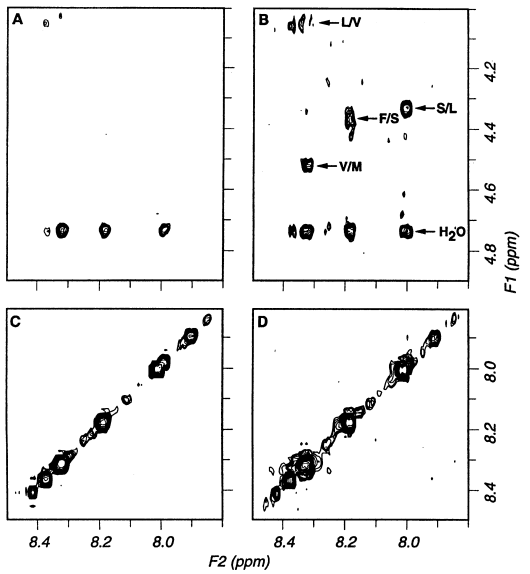

Figure 4. Parts of the NOESY spectrum of the peptide PapG308-314 by itself (A and C) and in the presence of PapD (B and D). The NH/Hα (A and B) and NH/NH (C and D) regions are shown. Strong sequential $H\alpha_i/NH_{i+1}$ TRNOEs were observed in the presence of PapD (marked in B with one letter codes for the corresponding amino acids in the peptide), whereas sequential NH_i/NH_{i+1} TRNOEs were absent (D), indicating that the peptide is bound in an extended, β-strand conformation. The spectra were plotted at equal threshold. Pulse field gradients were used for water suppression, explaining the presence of exchange peaks to water.

no cross peaks since the correlation time of the peptide is such that $\omega\tau_c \approx 1$, resulting in NOEs close to zero (Fig. 4A and C).[33] On addition of PapD ($Mw \approx 25$ kDa and thus $\omega\tau_c \gg 1$), to give a PapD-peptide ratio of 1:25, strong TRNOE peaks built up in the PapD-peptide complex were observed (Fig. 4B). TRNOEs were observed for both the *cis* and *trans* forms of PapG308-314 indicating the ability of PapD to bind both forms. In general, the TRNOEs for the *cis* form were much weaker, suggesting a weaker binding to PapD and consequently the *cis* form was discarded from further analysis. In the *trans* form strong sequential $H\alpha_i/NH_{i+1}$ TRNOEs were observed from Met^{309} through Phe^{313} (Fig. 4B). Sequential NH_i/NH_{i+1} TRNOEs could not be detected for PapG308-314 (Fig. 4D) and the sharp NH resonances observed for the peptide in the presence of PapD showed that this was not due to NH line broadening. Furthermore, weak intraresidue $H\alpha_i/NH_i$ TRNOEs could only be seen for residues Leu^{311} and Phe^{313}. Altogether, these TRNOEs indicate an extended conformation for PapG308-314 when bound by PapD.[26,27] Medium range TRNOEs were observed between the methyl groups of Val^{310} and the Hβ protons of Ser^{312}, as well as between the methyl groups of Leu^{311} and the aromatic ring protons of Phe^{313}. These medium range TRNOEs are also in agreement with an extended, β-strand structure for PapG308-314 in which the side chains of Val^{310} and Ser^{312} are on one side of the β-strand and those of Leu^{311} and Phe^{313} on the other. The possibilities that the medium range TRNOEs were due to spin diffusion could be ruled out, as discussed elsewhere in detail.[34] No intermolecular TRNOEs, between the ligand and the protein, were observed since the PapD concentration used in the experiment was too low to enable such observations.

TRNOEs may also originate from nonspecific binding of a ligand to a protein or because of an increase in the viscosity of the solution upon addition of the protein.[31] As a control, a NOESY spectrum was acquired for a solution of PapG308-314 and the protein calbinidin D_{28k}, which has a similar molecular weight as PapD, using a peptide-protein ratio of 10:1. The spectrum did not show any cross peaks indicating that the interaction between PapG308-314 and PapD is specific. Spin diffusion in large proteins, leading to intense cross peaks even for protons that are not close in space, is a well-known problem. The observed TRNOEs for PapG308-314 could, therefore, be affected by spin diffusion through protons of the protein. This type of indirect transfer of magnetization can be alleviated by keeping the fraction of bound peptide low[35] and a 25:1 ratio between PapG308-314 and PapD was therefore used.

The $^3J_{HN\alpha}$ coupling constants were determined for the complex between PapD and PapG307-314 to obtain further structural information on the complex. Owing to the ^{15}N labeling of the peptide the coupling constants could be determined from the intensity of the ^{15}N–Hα cross peaks in a set of constant-time HMQC experiments.[36] $^3J_{HN\alpha}$ values between 8.2 and 9.0 Hz were obtained for residues Val^{310} (8.6 ± 0.13 Hz), Leu^{311} (8.2 ± 0.13 Hz), Ser^{312} (8.4 ± 0.16 Hz), and Phe^{313} (9.0 ± 0.11 Hz) in the PapG307-314. These coupling constants correspond well with values found in β-strand regions of proteins (8.5 Hz),[37] clearly indicating that the PapG307-314 is bound in an extended conformation by PapD.

Further information on the mode of interaction of PapG308-314 with PapD was obtained from line broadening and differences in chemical shifts displayed by some proton resonances. Broadening of resonances is a consequence of large chemical shift differences between the free and bound form of the peptide. In the presence of PapD the Hβ resonances of Phe^{313} show a significant broadening as do the Hβ protons of Leu^{311} and Met^{309}, revealing these residues to contact PapD in the complex (Fig. 5A and B). These Hβ resonances also display significant differences in chemical shifts[38] in

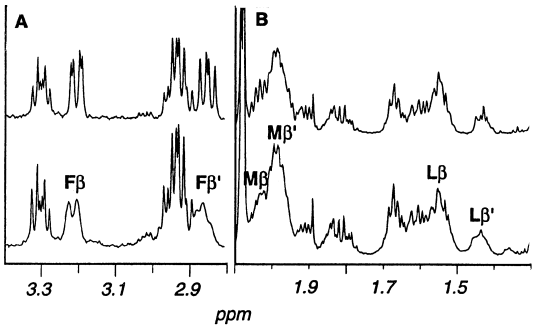

Figure 5. Selected parts of the one-dimendional ^{1}H NMR spectrum of the peptide PapG308-314 by itself (upper) and in the presence of PapD (lower). Resonances from Hβ of Met^{309}, Leu^{311} and Phe^{313} were broadened and shifted in the presence of PapD and have been marked with the one letter codes for the corresponding amino acid.

the presence and absence of PapD (Table 2). It should be noted that the side chains of Phe^{313}, Leu^{311}, and Met^{309} were also those found to make the most important contacts with PapD in the inhibition ELISA. In addition, broadening of backbone resonances, as well as chemical shift differences (Table 2), were observed in the one-dimensional proton spectrum and in the TOCSY spectrum for several resonances from Leu^{311} and Ser^{312} when PapD was added. Most likely, the backbone in the center of PapG308-314 is bound more rigidly by PapD, as compared to the N- and C-terminus, explaining these line broadening effects and chemical shift differences.

Discussion

Periplasmic chaperones are required for assembly of pili which mediate binding to host tissue in a large number of pathogenic, gram-negative bacteria.[1] Since interference with pilus assembly reduces bacterial virulence, compounds that inhibit chaperone function may constitute novel antibiotics. Chaperones involved in pilus assembly show significant homology to PapD,[2,14] which mediates pilus assembly in uropathogenic *E. coli*. This suggests that all periplasmic chaperones have structures closely related to that determined for PapD[13] and, furthermore, that chaperone-inhibitors could have a broad spectrum. In the present investigation an ELISA in which peptides, or other compounds, may be evaluated as inhibitors of the binding of PapD to the MaltBP–PapG175-314 fusion protein[16] has been developed. The complex between PapD and MaltBP–PapG175-314 has previously been shown to be as stable as the native PapD–PapG complex,[16] arguing that the ELISA is a relevant model for the function of PapD, in particular, and other chaperones in general. The ELISA has been used to evaluate the inhibitory power of a set of synthetic peptides related to P pilus proteins. It should also prove useful for screening of chemical libraries prepared by combinatorial chemistry,[39–41] or for optimization of lead compounds.

When evaluated in the inhibition ELISA, the C-terminal 19-mer peptides PapG296-314 and PapH155-173, which are derived from the pilus adhesin PapG and anchor PapH, respectively, were both found to be potent inhibitors of formation of the PapD–PapG complex. In contrast, the C-terminal 19-mer peptides from PapF, E, and K, which make up the pilus tip, did not show any significant inhibitory power, even when evaluated at a 200-fold excess as compared to PapD. It is possible that the superior inhibitory power of the PapG and PapH peptides reflect the critical functions that the corresponding proteins have for initiation and termination of pilus assembly, respectively. The high inhibition obtained for PapG296-314 agrees well with the high affinity displayed by PapD for this peptide when it was coated in microtiter plate wells, or when used to inhibit PapD mediated folding of denatured PapG.[15] However, PapH155-173 adsorbed to microtiter plate wells did not bind the PapD chaperone,[15] indicating the importance of using several bioassays when screening ligands for binding to macromolecules. The 19-mer PapG296-314 could be N-terminally truncated to the octapeptide PapG307-314 without a major loss of inhibitory power in the ELISA, revealing that PapG307-314 provides most of the interactions between PapD and C-terminal peptides from PapG. These results are in good overall agreement with the structure of the crystalline complex between PapD and PapG296-314, in which the peptide extends one of the β-sheets in PapD by hydrogen bonding and side-chain interactions involving the eight C-terminal residues of the peptide.[15] In the crystal, Met^{307}, which is the first of these eight residues, contributes two of the nine backbone-to-backbone hydrogen bonds to PapD. The observations that truncation of Met^{307} from PapG307-314 led to a significantly reduced inhibitory power, whereas replacement of this residue with Ala or Ser had no such effect, confirmed the importance of backbone-to-backbone hydrogen bonding for stabilization of PapD-peptide complexes also in solution. Truncation of PapH155-173, either at the N-terminus or at the C-terminus, abolished inhibition in the ELISA. This suggests that conformational preferences may be important for binding of PapH155-173 to PapD, or that this peptide binds in a different way, or to a different part of PapD than the PapG peptides. Since limited solubility and tendencies to form aggregates influenced the inhibitory power of at least two of the five 19-mer peptides, the C-terminal octapeptides

from the six pilus proteins were also evaluated in the ELISA. Apart from PapG307-314, and possibly PapK150-157, none of the octapeptides were able to inhibit binding of PapD to MaltBP–PapG175-314. It should, however, be pointed out that amino acid residues in the pilus proteins PapA and PapE, that were located within the peptides employed in the present investigation, have been found to be essential for subunit binding to PapD.[12]

The importance of individual side chains in the minimal inhibitory peptide from PapG (PapG307-314) for binding to PapD in solution was investigated using both an alanine and a serine scan peptide series. It was found that substitution with serine, in addition to alanine, substantially facilitated interpretation of the results obtained in the inhibition ELISA. Comparison of the inhibitory powers of the members of the two series with that of PapG307-314 revealed that the side chains of Met^{309}, Leu^{311}, and Phe^{313} provided important contacts to PapD. The remaining five side chains could all be replaced without any major influence on the inhibitory power. Furthermore, line broadening and chemical shift differences were observed for the β-protons of Met^{309}, Leu^{311}, and Phe^{313} in the ^1H NMR spectrum of PapG308-314 on addition of PapD, confirming that these residues contact PapD in aqueous solution. In the crystalline complex between PapD and PapG296-314 the side chains of these three residues, as well as that of Met^{307}, were found to contribute 20% of the total buried surface area between peptide and protein.[15] As revealed by the inhibition studies the side chain of Met^{307} is less important; an observation which agrees well with the fact that four out of the six pilus proteins have an alanine at this position (cf. Table 1). In contrast, all P pilus proteins have large hydrophobic side chains at the positions corresponding to Met^{309}, Leu^{311}, and Phe^{313}.

Inspection of the crystalline complex between PapD and the peptide PapG296-314 suggested that formation of a salt bridge between the C-terminal carboxyl group of the peptide and the invariant residues Arg^8 and Lys^{112} in PapD was essential for complex formation.[15] However, in solution, the ability of peptides to form this salt bridge was not critical for inhibition of PapD–PapG complex formation. This conclusion was based on the fact that peptides from PapG in which Pro^{314} had been deleted, or in which the α-carboxyl group had been reduced to a methyl group, retained all or most of their inhibitory power. At first this appears to be in conflict with previous results showing that site-specific mutation of Arg^8 or Lys^{112} in PapD abolished the ability of PapD to bind to pilus proteins and mediate pilus assembly in vivo.[15] However, in pilus protein–PapD complexes, the salt bridge is most likely deeply buried and deletion of one of its components can then be expected[42] to have a drastic influence on the stability of the complex. In contrast, in a PapD–peptide complex, the residues are located on the surface of the complex allowing interactions with the aqueous environment to compensate for loss of the salt bridge.

^1H NMR spectroscopy was used in an attempt to establish if different conformational propensities played a role in determining the ability of the pilus derived 19-mer peptides to inhibit binding of PapD to the MaltBP–PapG175-314 fusion protein. Due to the low solubility of the peptides in aqueous solution, the NMR studies were performed in DMSO, which was also used as the cosolvent in the inhibition ELISA. Inspection of NOEs, $^3J_{NH\alpha}$ coupling constants and chemical shifts indicated that the 19-mer peptides behaved as random coils in DMSO solution. This conclusion was also reached in a previous NMR study of PapG296-314 performed in aqueous solution.[18] However, conformational studies of PapG296-314 carried out in different solutions using CD spectroscopy have revealed[18] that the peptide does have a significant propensity to adopt a β-strand structure, i.e. the conformation adopted in the crystalline complex with PapD. In contrast, the conformations of PapF130-148, PapE131-149, and PapK139-157 appeared to be influenced by the surrounding environment to a much larger extent.[18] The preference for adopting a β-strand structure may therefore provide part of the explanation for the high ability of PapG296-314 to bind to and inhibit PapD.

The conformation of C-terminal hepta- and octapeptides from PapG, when bound by PapD, was investigated in solution using both transferred nuclear Overhauser effect spectroscopy (TRNOE) and isotope edited NMR spectroscopy. The observation of strong sequential $H\alpha_i/NH_{i+1}$ TRNOEs along the backbone of the peptides and the absence of sequential NH_i/NH_{i+1} TRNOEs indicated that the peptides were bound by PapD in an extended, β-strand like conformation. This conclusion was further supported by TRNOEs revealing that the side chains of Val^{310} and Ser^{312} are on one side of the β-strand and those of Leu^{311} and Phe^{313} on the other. In addition, the $^3J_{NH\alpha}$ coupling constants obtained for ^{15}N-labeled PapG307-314 were between 8.2 and 9.0 Hz, i.e. close to those found in β-strand regions of proteins.[37] NMR spectroscopy, therefore, revealed that peptides from PapG are bound in the same conformation by PapD as in the crystal. It should, however, be pointed out that the peptides used in the NMR studies are too short to allow formation of the dimers found in the crystal and that dimerization was previously excluded[34] using asymmetrical field-flow fractionation.

The information obtained by evaluation of peptides as inhibitors of PapD–PapG complex formation, together with that from NMR studies of peptide–PapD complexes, thus provided a coherent picture of how PapD binds peptides from the adhesin PapG in solution. With only two exceptions, this picture is in good agreement with the structure in the crystalline complex of PapD and the longer peptide PapG296-314.[15] Importantly, the present investigation reveals that the structure of the complex was not significantly influenced by the dimerization present in the crystal. The crystal structure, in combination with the present solution studies, may therefore be used as a starting point in efforts to design compounds that inhibit pilus assembly in pathogenic bacteria. Evaluation of such chaperone inhibitors should be facilitated by using the inhibition ELISA developed by us.

Conclusions

Bacterial periplasmic chaperones, such as PapD in *E. coli*, bind the protein subunits that make up adhesive pili and incorporate them into the functional pilus. An ELISA has now been developed which allows evaluation of compounds as inhibitors of complex formation between PapD and the pilus adhesin PapG. Evaluation of peptides from the C-terminus of the six proteins that make up the *E. coli* P pilus, revealed that peptides from the adhesin PapG were the most potent PapD inhibitors and that most of the inhibitory activity was retained in the C-terminal octapeptide PapG307-314. NMR spectroscopy of the complexes between PapD and PapG307-314, or PapG308-314, revealed that the peptides were bound as extended β-strands by PapD in aqueous solution. Furthermore, evaluation of a panel of analogues of PapG307-314 in the ELISA, as well as further NMR studies, showed that the complex was stabilized by backbone-to-backbone hydrogen bonds and interactions involving the hydrophobic side chains of Met^{309}, Leu^{311}, and Phe^{313} of the peptide. Most likely, a preference for adopting a β-strand structure also improved peptide binding to PapD. The structure deduced for the complex between PapD and the PapG307-314 peptide in aqueous solution is, with some exceptions, in good agreement with the structure determined for the crystalline complex of PapD bound to the 19-mer peptide PapG296-314. This structural information may be used in efforts to design and synthesize compounds that inhibit periplasmic chaperones in pathogenic bacteria.

Experimental

Abbreviations used: Boc: *tert*-butoxycarbonyl; CHAPS: 3-[(3-cholamidopropyl)dimethylammonio]-1-propanesulfonate; COSY: correlated spectroscopy; DIPSI: decoupling in the presence of scalar interactions; ELISA: enzyme linked immunosorbent assay; HATU: *O*-(7-azabenzotriazol-1-yl)-1,1,3,3-tetramethyluronium hexafluorophosphate; HETCOR: heteronuclear correlation spectroscopy; HMQC: heteronuclear multiple quantum coherence spectroscopy; HOAt: 1-hydroxy-7-azabenzotriazole; HSQC: heteronuclear single quantum coherence spectroscopy; MaltBP: maltose binding protein; NMM: *N*-methylmorpholine; NOESY: nuclear Overhauser effect spectroscopy; Pap: pyelonephritis-associated pilus; ROESY: rotating frame nuclear Overhauser effect spectroscopy; TBTU: *O*-(benzotriazol-1-yl)-1,1,3,3-tetramethyluronium tetrafluoroborate; TOCSY: total correlation spectroscopy; TRNOE: transferred nuclear Overhauser effect.

General methods and materials

TLC was performed on Silica Gel 60 F_{254} (Merck, Germany) with detection by UV light. Flash column chromatography was performed on silica gel (Matrex, 60 Å, 35–70 μm, Grace Amicon, U.S.A.) with distilled solvents. DMF was dried by distillation and kept over molecular sieves (4 Å). Organic solutions were dried over Na_2SO_4 before being concentrated. ^1H and ^{13}C NMR spectra were recorded at 400 and 100 MHz, respectively, at 300 K. Residual $CHCl_3$ (δ_H 7.25 ppm) and $CDCl_3$ (δ_C 77.0 ppm) were used as internal standards. First-order chemical shifts and coupling constants were obtained from one-dimensional spectra. Assignments of resonances were based on COSY and HETCOR experiments. Ions for positive fast-atom bombardment mass spectra were produced by a beam of Xenon atoms (6 keV) from a matrix of glycerol and thioglycerol. Analytical reversed-phase HPLC was performed on a Kromasil C-8 column (100 Å, 5 μm, 4.6×250 mm, Hichrom Ltd., U.K.) using a linear gradient of 0→80% ***B*** in ***A*** over 60 min with a flow rate of 1.5 mL/min and detection at 214 nm (solvent systems ***A***: 0.1% aqueous trifluoroacetic acid and ***B***: 0.1% trifluoroacetic acid in CH_3CN). Preparative reversed-phase HPLC was performed on a Kromasil C-8 column (100 Å, 5 μm, 20×250 mm, Hichrom Ltd., U.K.) using the same eluent and a flow rate of 10 mL/min.

***N*$^{\alpha}$-*tert*-Butoxycarbonyl-L-phenylalanine (2*S*)-hydroxymethylpyrrolidinyl amide (3).** L-Prolinol (**2**, 137 mg, 1.36 mmol) and *N*-methylmorpholine (NMM) (343 mg, 3.39 mmol) were added to a solution of N^{α}-*tert*-butoxycarbonyl-L-phenylalanine (**1**, 300 mg, 1.13 mmol) and 2-(1H-benzotriazol-1-yl)-1,1,3,3-tetramethyluronium tetrafluoroborate (TBTU) (436 mg, 1.36 mmol) in DMF (6 mL) and the mixture was stirred at room temperature for 5 h under nitrogen. The mixture was diluted with EtOAc (20 mL) and washed with saturated aqueous

NH_4Cl (2×20 mL) and saturated aqueous $NaHCO_3$ (2×20 mL). The organic phase was dried, filtered, and concentrated. Flash column chromatography (heptane/EtOAc, 1/1) of the residue gave **3** (303 mg, 77%): $[\alpha]_D^{25}$ 0° (*c* 1.40, $CHCl_3$); ^1H NMR ($CDCl_3$), amide bond rotamer ratio 4:1, δ 7.33–7.20 (m, 5 H, Ph), 5.38 (bd, $J=9.1$ Hz, 0.8 H, *trans*-Phe NH), 5.35 (bd, $J=10.3$ Hz, 0.2 H, *cis*-Phe NH), 4.81 (dt, $J=8.8$, 6.0 Hz, 0.2 H, *cis*-Phe Hα), 4.66 (dt, $J=9.0$, 5.5 Hz, 0.8 H, *trans*-Phe Hα), 4.35 (bs, 0.8 H, *trans*-pyr OH), 4.20–4.12 (m, 0.8 H, *trans*-pyr Hα), 3.92 (bs, 0.2 H, *cis*-pyr OH), 3.62–3.51 (m, 1.6 H, *trans*-Phe Hδ, *trans*-pyr CH_2O), 3.51–3.34 (m, 1.6 H, *trans*-Phe CH_2O, *cis*-pyr Hδ,δ, *cis*-pyr CH_2O), 3.34–3.27 (m, 0.2 H, *cis*-pyr Hα), 3.09–2.88 (m, 2 H, Phe Hβ), 2.63 (dt, $J=10.0$, 7.2 Hz, 0.8 H, *trans*-pyr Hδ), 1.99–1.89 (m, 0.8 H, *trans*-pyr Hβ), 1.76–1.57 (m, 2 H, pyr Hγ), 1.50–1.37 (m, 9.8 H, Phe NBoc, *trans*-pyr Hβ), 1.29–1.24 (m, Phe NBoc rotamer), 1.20–1.06 (m, 0.4 H, *cis*-pyr Hβ,β); ^{13}C NMR ($CDCl_3$) δ 173.0, 155.5, 136.6, 130.0, 129.8, 129.0, 128.9, 127.5, 80.3, 67.1, 61.8, 54.0, 48.3, 40.7, 28.8, 28.7, 28.3, 24.7, 22.2; HRMS–FAB: ($M+H^+$) calcd for $C_{19}H_{28}O_4N_2$, 349.2127; found, 349.2137.

***N*$^{\alpha}$-*tert*-Butoxycarbonyl-L-phenylalanine (2*S*)-iodomethylpyrrolidinyl amide (4).** Compound **3** (200 mg, 0.57 mmol), iodine (364 mg, 1.44 mmol), triphenylphosphine (376 mg, 1.44 mmol), and imidazole (137 mg, 2.01 mmol) were stirred in toluene (20 mL) for 1.5 h at 80 °C. The mixture was diluted with toluene (25 mL) and the solid residue was dissolved in acetone (3 mL). The combined organic phase was washed with saturated aqueous $NaHCO_3$ (2×15 mL) and H_2O (2×15 mL), dried, filtered, and concentrated. Flash column chromatography (heptane/EtOAc, 4/1) of the residue gave **4** (168 mg, 64%): $[\alpha]_D^{25}$ +18° (*c* 1.21, $CHCl_3$); ^1H NMR ($CDCl_3$), amide bond rotamer ratio 5:2, δ 7.34–7.20 (m, 5 H, Phe Ph), 5.32 (bd, $J=8.2$ Hz, 1 H, Phe NH), 4.63 (dt, $J=7.7$, 7.7 Hz, 0.7 H, *trans*-Phe Hα), 4.58–4.51 (m, 0.3 H, *cis*-Phe Hα), 4.20–4.13 (m, 0.7 H, *trans*-pyr Hα), 3.62–3.52 (m, 1H, pyr Hδ), 3.47 (dd, $J=9.5$, 2.8 Hz, 1 H, pyr CH_2I), 3.36–3.25 (m, 0.3 H, *cis*-pyr Hα), 3.07–2.88 (m, 4 H, Phe Hβ,β, pyr Hδ, pyr CH_2I), 2.08–1.95 (m, 1 H, pyr Hβ), 1.89–1.74 (m, 3 H, pyr Hβ, pyr Hγ,γ), 1.45 (s, 2.7 H, *cis*-Phe NBoc), 1.41 (s, 6.3 H, *trans*-Phe NBoc), 1.27 (s, Phe NBoc rotamer); ^{13}C NMR ($CDCl_3$) δ 171.1, 155.5, 136.8, 130.0, 129.8, 129.0, 128.8, 127.5, 127.4, 80.2, 58.5, 53.7, 48.0, 46.4, 40.4, 30.8, 28.8, 24.3, 9.2; HRMS–FAB: ($M+H^+$) calcd for $C_{19}H_{27}O_3N_2I$, 459.1145; found, 459.1163.

***N*$^{\alpha}$-*tert*-Butoxycarbonyl-L-phenylalanine (2*R*)-methylpyrrolidinyl amide (5).** Compound **4** (84 mg, 0.18 mmol) and triethylamine (32 μL, 0.23 mmol) were dissolved in EtOAc (1 mL) and EtOH (5 mL) and 10% Pd/C (50 mg) was then added under argon. The reaction mixture was hydrogenated at 1 atm for 1 h and 10 min, then filtered through Celite, which was washed with CH_2Cl_2 and EtOH. The combined filtrates were concentrated and the residue was dissolved in CH_2Cl_2 (20 mL). The solution was washed with H_2O (10 mL), dried, filtered, and concentrated. Flash column chromatography (heptane/acetone, 6/1) of the residue gave **5** (57 mg, 93%): $[\alpha]_D^{25}$ +6° (*c* 1.30, $CHCl_3$); ^1H NMR ($CDCl_3$), amide bond rotamer ratio 5:3, δ 7.30–7.19 (m, 5 H, Phe Ph), 5.43 (bd, $J=7.7$ Hz, 1 H, Phe NH), 4.66 (dt, $J=9.6$, 5.1 Hz, 0.4 H, *cis*-Phe Hα), 4.57 (dt, $J=8.7$, 5.7 Hz, 0.6 H, *trans*-Phe Hα), 4.21–4.11 (m, 0.6 H, *trans*-pyr Hα), 3.46 (ddd, $J=11.7$, 9.4, 2.5 Hz, 0.4 H, *cis*-pyr Hδ), 3.42–3.33 (m, 0.6 H, *trans*-pyr Hδ), 3.30–3.18 (m, 0.8 H, *cis*-pyr Hα, *cis*-pyr Hδ), 3.07–2.88 (m, 2 H, Phe Hβ), 2.75–2.65 (m, 0.6 H, *trans*-Phe Hδ), 1.94–1.83 (m, 0.6 H, *trans*-Phe Hβ), 1.74–1.64 (m, 1 H, pyr Hγ), 1.45–1.37 (m, 10.4 H, Phe NBoc, *trans*-pyr Hβ, *cis*-pyr Hβ), 1.31–1.21 (m, Phe NBoc rotamer), 1.09 (2 d, each $J=3.1$ Hz, 3 H, pyr Me); ^{13}C NMR ($CDCl_3$) δ 170.0, 155.5, 136.9, 130.1, 129.8, 128.8, 128.7, 127.2, 80.0, 53.8, 53.5, 53.3, 46.9, 45.5, 41.5, 40.7, 32.8, 32.1, 28.8, 28.8, 24.3, 21.9, 21.5, 19.6; HRMS–FAB: ($M+H^+$) calcd for $C_{19}H_{28}O_3N_2$, 333.2178; found, 333.2282.

***N*$^{\alpha}$-9-Fluorenylmethoxycarbonyl-L-methionyl-L-threonyl-L-methionyl-L-valyl-L-leucyl-L-serine (6).** Peptide fragment **6** was synthesized on PEG-PS resin (TentaGel S PHB Ser(t-Bu) Fmoc resin, 0.21 mmol/g, 300 mg) as described below in the general section on peptide synthesis. The crude product (33 mg) was purified by reversed-phase preparative HPLC to give **6** (7 mg, 12%); MS–FAB: ($M+H^+$) calcd, 903; found, 903.

***N*$^{\alpha}$-9-Fluorenylmethoxycarbonyl-L-methionyl-L-threonyl-L-methionyl-L-valyl-L-leucyl-L-seryl-L-phenylalanine (2*R*)-methylpyrrolidinyl amide (7).** The *N*$^{\alpha}$-*tert*-butoxycarbonyl group was removed from **5** (4 mg, 12 μmol) by treatment with a solution of HCl in acetic acid (1 M, 400 μL) for 1 h. Portions of CH_2Cl_2 (5×1 mL) were added to the solution and then removed by concentration. The residue was dissolved in DMF (150 μL), then peptide fragment **6** (5.2 mg, 6 μmol), HATU (46 μL of a 0.26 M solution in DMF, 12 μmol) and HOAt (32 μL of a 0.37 M solution in DMF, 12 μmol) were added. The solution was cooled to 0 °C and trimethylpyridine (TMP, 80 μL of a 0.45 M solution in DMF, 36 μmol) was added. The coupling was monitored by analytical reversed-phase HPLC. After 1 h at 0 °C and 2 h at room temperature, purification (without prior work up) was performed by preparative reversed-phase HPLC to give **7** (3.38 mg, 53%); MS–FAB: ($M+H^+$) calcd, 1117; found, 1117.

L-Methionyl-L-threonyl-L-methionyl-L-valyl-L-leucyl-L-seryl-L-phenylalanine (2*R*)-methylpyrrolidinyl amide (8). Peptide **7** (2.3 mg, 2 μmol) was dissolved in a solution

of piperidine in DMF (20%, 300 μL) at room temperature and the reaction was monitored by analytical reversed-phase HPLC. After 1 h, purification (without prior work up) was performed by preparative reversed-phase HPLC to give **8** (0.68 mg, 26%); MS–FAB: $(M+H^+)$ calcd, 895; found, 895.

Peptide synthesis

Synthesis, purification, and characterization of the peptides PapG296-314, PapF130-148, PapE131-149, PapK139-157, and PapH155-173 have been described elsewhere.[18] All other peptides used in this study were prepared in the same manner by the 9-fluorenylmethoxycarbonyl (Fmoc) solid-phase synthesis strategy using a fully automated continuous flow peptide synthesizer, constructed in our laboratory essentially as described previously by others.[19] Synthesis was performed on a polystyrene resin grafted with polyethylene-glycol spacers (TentaGel PEG-PS resin, Rapp Polymere, Germany) using commercially available N^{α}-Fmoc amino acids carrying standard side-chain protective groups (Bachem, Switzerland). All but two peptides (PapG299-306 and PapH155-165) were synthesized as C-terminal carboxylic acids on resins functionalized with a 4-alkoxybenzyl alcohol linker and the appropriate C-terminal amino acid or a 2-chlorotrityl linker[43] and Fmoc-proline. The peptides PapG299-306 and PapH155-165 were instead prepared as C-terminal amides using the Rink linker, *p*-[α-(fluoren-9-ylmethoxyformamido)-2,4-dimethoxybenzyl]phenoxyacetic acid.[44,45] ^{15}N-Labelled amino acids (^{15}N, 95–99%, CIL, U.S.A.) were protected with an N^{α}-Fmoc group prior to their use in synthesis. After TFA-catalyzed cleavage from the resin, the peptides were purified to greater than 95% homogeneity by reversed-phase HPLC and molecular weights were confirmed by FABMS.

Peptide inhibition ELISA

Microtiter plate wells (Nunc-Immuno Plate Maxisorp, Denmark) were each coated with a solution of the MaltBP–PapG175-314 fusion protein (50 μL at 10 pmol/50 μL) in PBS (138 mM NaCl, 2.7 mM KCl, 8.2 mM phosphate, pH 7.4) for 24 h at 4 °C. The solutions in the wells were discarded. The wells were each blocked with a solution of 3% BSA (Sigma, U.S.A.) in PBS (200 μL) for 2–3 h at 25 °C: the plates were then washed vigorously three times with PBS. The peptide to be evaluated was dissolved to six different concentrations (600, 300, 150, 38, 9, and 2 μM) in DMSO (Fluka, Switzerland). Each peptide solution (10 μL) was pre-incubated with a solution of PapD (10 μL at 30 pmol/10 μL) in KMES buffer (20 mM potassium 2-(*N*-morpholino)-ethanesulfonate, pH 6.5) for 2 h at 25 °C. The PapD–peptide solution was diluted 50 times with PBS containing 0.05% Tween® 20 (polyoxyethylene sorbitanmonolaurate, Fluka, Switzerland) and 50 μL of the resulting solution was added, in triplicate, to the coated wells and incubated at 25 °C for 2 h. The plates were washed three times with PBS and the wells were incubated with a solution of rabbit antiserum to PapD in PBS containing 3% BSA (1:1000 dilution, 50 μL) for 2 h at 25 °C. The plates were again washed three times with PBS and the wells were incubated with a solution of goat antiserum to rabbit IgG coupled to alkaline phosphatase (Sigma, U.S.A.) in PBS containing 3% BSA (1:1000 dilution, 50 μL) for 2 h at 25 °C. After three washings with PBS and three washings with developing buffer (10 mM diethanolamine, 0.5 mM $MgCl_2$, pH 9.5), filtered *p*-nitrophenyl phosphate (Sigma, U.S.A.) in developing buffer (10 mg/mL, 50 μL) was added to each well and incubated for 30 min in the dark at 25 °C. The absorbance at 405 nm was read and the per cent inhibition was calculated by dividing the amount of PapD binding to the coated MaltBP–PapG175-314 fusion protein in the presence of peptide with the amount of PapD binding in the absence of peptide, and subtracting the ratio from 1. The per cent inhibition (Inhibitory Power) represents the average of three experiments, each performed in triplicate. From these the standard deviation (SD) was calculated and 95% confidence intervals were obtained as:

$$\text{Inhibitory Power} \pm \text{SD} \cdot 1.96\sqrt{n}$$

$$\text{where SD} = \sqrt{\frac{1}{n-1}\sum_{i=1}^{n}(\bar{x}-x_i)^2}$$

and where $n = 3$ and $\bar{x}$ is the mean of the values for the Inhibitory Power (x_i).

In the ELISA maximum binding of PapD to the MaltBP–PapG175-314 coated wells was obtained in the absence of peptide (but with DMSO still present). This maximum binding value was used in calculation of the Inhibitory Power as described above. Since fluctuation was observed for the Inhibitory Powers of the peptides, the fluctuation of the maximum binding value was also determined. This was done from five randomly chosen microtiter plates, each of which gave four values for the maximum binding value. It was found that the average of the SD of the maximum binding value divided by the maximum binding value was 8.5%, with a SD of 4.84%.

NMR spectroscopy of PapG296-314, PapE131-149, PapK139-157, and PapH155-173

PapG296–314, PapE131-149, PapK139-157, and PapH155-173 were dissolved in DMSO-d_6 (99.9%, Glaser AG, Switzerland) at a concentration of 3.0, 2.1,

0.6, and 0.5 mM, respectively. Phase sensitive COSY,[46,47] TOCSY,[48–50] NOESY,[51–53] and ROESY[54,55] spectra were acquired at 500 MHz and at 27 °C. The DMSO-d_6 resonance at 2.50 ppm was used as internal shift reference. TOCSY experiments were performed using the modification suggested by Rance[56] and the dipsi-2 mixing sequence[57] using a spin-lock period of 100 ms. Mixing times of 100–200 ms were used in the ROESY and NOESY (PapH155-173) experiments. All spectra were recorded in the phase sensitive mode[58] with 512 t_1 increments and 4096 complex data points in t_2. After zero filling, the final size of the data matrices was 1024×2048 points. Data were processed on a Sun Sparc workstation (PapH155-173) using the FELIX software (Biosym Technologies, U.S.A.) or on a Silicon Graphics INDY workstation (PapG296-314, PapE131-149, and PapK139–157) using the XWIN-NMR software (Bruker, Germany). Determination of $^3J_{HN\alpha}$ coupling constants (PapH155-173) were made in a resolution-enhanced COSY spectrum, zero-filled to give a 0.7 Hz/point digital resolution in ω2.

TRNOE study of the PapD–PapG308-314 complex

Three identical samples were prepared for NMR spectroscopy by dissolving PapG308-314 to a concentration of 0.5 mM in 50 mM phosphate buffer, pH 6.0, containing 10% D_O and 0.02% NaN_3 (the low solubility of PapG308-314 prevented use of a higher concentration). A stock solution of PapD[13] in PBS (~70 μM, pH 7.4) was concentrated to 200 μM by centrifugation in an Ultrafree micro concentrator (cut-off = 5 kDa, Millipore, U.S.A.) prior to dilution into one of the PapG308-314 samples. The resulting PapD concentration was 20 μM giving a PapG308-314–PapD ratio of 25:1. A control sample was prepared by dissolving lyophilized Calbindin D_{28k}[59] into another of the PapG308-314 samples to give a PapG308-314–Calbindin D_{28k} ratio of 10:1. No additions were made to the third PapG308-314 solution. Phase sensitive NOESY,[51,52] ROESY,[54,55] and TOCSY[48] spectra were acquired at 600 MHz and 27 °C using the water resonance at 4.75 ppm as internal shift reference. Presaturation was used to attenuate the water signal except in the NOESY experiments where pulse field gradients were used for water suppression. The WATERGATE-NOESY pulse sequence[60] was modified as described.[61] NOESY spectra were acquired with mixing times of 20, 200, and 500 ms and ROESY spectra were acquired with a continuous wave spin-lock mixing time of 200 ms. The TOCSY experiments, modified as described above for the 19-mer peptides, were recorded with a spin-lock period of 90 ms. All spectra were recorded using the hypercomplex method[58] with 400 t_1 increments and 2048 complex data points in t_2. After zero filling, the final size of the data matrixes were 1024×2048. Data were processed on a Sun Sparc workstation using the FELIX software (Biosym Technologies, U.S.A.). One-dimensional spectra were acquired with 512 scans, 16 k complex data points, and presaturation.

3D-NOESY-HSQC study of the complex between PapD and ^{15}N-labelled PapG307-314

A stock solution of PapD[13] in PBS (~0.3 mM, pH 7.4) was diluted in PBS (pH 6.0) and concentrated to a final concentration of 0.6 mM using a Centricon 10 micro concentrator (cut-off = 10 kDa, Amicon, U.S.A.). PapG307-314 was dissolved in DMSO-d_6 (20 μL) and added to the PapD solution to give a PapG307-314–PapD ratio of 1:1. A sensitivity enhanced 2-D ^{15}N-HSQC spectrum with gradient selection,[62] a 2-D ^{15}N-HSQC–TOCSY spectrum[62] with a DIPSI-2 relaxation compensated isotropic mixing sequence,[63] and a 3-D ^{15}N-NOESY-HSQC spectrum[62] were acquired at 600 MHz and 27 °C. Water-flip-back pulses were used to suppress the water signal. Mixing times of 80 and 100 ms were used in the heteronuclear TOCSY and NOESY experiments, respectively. A spectral width of 7490 Hz was used in the ^{1}H dimension of all experiments. The HSQC experiment was recorded with a spectral width of 1600 Hz in the ^{15}N dimension and with 128 scans, 128 t_1 increments, and 2048 complex data points in t_2. The HSQC-TOCSY and NOESY-HSQC experiments were acquired with a spectral width of 1000 Hz in the ^{15}N dimension. The HSQC-TOCSY experiment was recorded with 256 scans, 128 t_1 increments, and 1024 complex data points in t_2. In the NOESY-HSQC experiment 128 t_1 increments, 32 t_2 increments and 1024 complex data points in t_3 were acquired collecting 12 scans for each t_1 and t_2 point. $^3J_{HN\alpha}$ coupling constants were determined from six constant-time 2-D HMQC experiments[36] recorded with 45, 60, 80, 100, 120, and 140 ms dephasing times. The spectra were recorded with 1024 complex data points in t_2 and 64 scans for each of the 64 t_1 points using the same spectral widths as used in the HSQC-TOCSY experiment. Linear prediction was applied to all spectra in order to increase the spectral resolution. Cross peak intensities at various dephasing times were fitted against the following equation

$$\mathbf{I}_y(t) = \mathbf{I}_y(0)\mathbf{N}_1 \exp[-t/T_2 - t/(2T_1)] \{\cos(\pi \mathbf{J}^r t) + \sin(\pi \mathbf{J}^r t)/(2\pi \mathbf{J}^r t)\}$$

with $\mathbf{J}^r = \sqrt{J^2_{HH} - 1/(2\pi T_1)^2}$, where N_1 is the number of t_1 increments in the constant-time dimension, t the dephasing time, T_2 the transverse relaxation rate, T_1 the selective longitudinal relaxation rate of the Hα protons and J_{HH} the $^3J_{HN\alpha}$ coupling constant. A uniform value of T_1 for the Hα protons was assumed to be 0.2 s. The

value of J_{HH} was optimized together with T_2. Data were processed on a Sun Sparc workstation using the FELIX software (Biosym Technologies, U.S.A.).

Acknowledgements

The authors are grateful to C. Pongratz for statistical analysis of the ELISA data for the pilus subunit derived 19-mer peptides, S. Linse for the gift of Calbindin D_{28k}, G. Carlström for pulse sequence programming (TRNOE) and G. Carlström and J. Evenäs for help with the 3-D-NOESY-HSQC NMR experiments. This work was funded by the Swedish National Board for Industrial and Technical Development and by the Swedish Natural Science Research Council.

Supplementary material

400 MHz ^{1}H NMR spectra and 100 MHz ^{13}C NMR spectra for compounds **3–5**. Tabulated 500 MHz ^{1}H NMR data for the peptides PapG296-314, PapE131-149, PapK139-157, and PapH155-173.

References and Notes

1. Hultgren, S. J.; Abraham, S.; Caparon, M.; Falk, P.; St. Geme, J. W., III; Normark, S. *Cell* **1993**, *73*, 887.

2. Hung, D. L.; Knight, S. D.; Woods, R. M.; Pinkner, J. S.; Hultgren, S. J. *EMBO J*. **1996**, *15*, 3792.

3. Kuehn, M. J.; Heuser, J.; Normark, S.; Hultgren, S. J. *Nature* **1992**, *356*, 252.

4. Bullitt, E.; Makowski, L. *Nature* **1995**, *373*, 164.

5. Källenius, G.; Möllby, R.; Svenson, S. B.; Winberg, J.; Lundblad, A.; Svensson, S.; Cedergren, B. *FEMS Lett*. **1980**, *7*, 297.

6. Leffler, H.; Svanborg Edén, C. *FEMS Lett*. **1980**, *8*, 127.

7. Kihlberg, J.; Hultgren, S. J.; Normark, S.; Magnusson, G. *J. Am. Chem. Soc*. **1989**, *111*, 6364.

8. Striker, R.; Nilsson, U.; Stonecipher, A.; Magnusson, G.; Hultgren, S. J. *Mol. Microbiol*. **1995**, *16*, 1021.

9. Nilsson, U.; Striker, R. T.; Hultgren, S. J.; Magnusson, G. *Bioorg. Med. Chem*. **1996**, *4*, 1809.

10. Hultgren, S. J.; Lindberg, F.; Magnusson, G.; Kihlberg, J.; Tennent, J. M.; Normark, S. *Proc. Natl. Acad. Sci. U.S.A*. **1989**, *86*, 4357.

11. Kuehn, M. J.; Normark, S.; Hultgren, S. J. *Proc. Natl. Acad. Sci. U.S.A*. **1991**, *88*, 10586.

12. Bullitt, E.; Jones, C. H.; Striker, R.; Soto, G.; Jacob-Dubuisson, F.; Pinkner, J.; Wick, M. J.; Makowski, L.; Hultgren, S. J. *Proc. Natl. Acad. Sci. U.S.A*. **1996**, *93*, 12890.

13. Holmgren, A.; Brändén, C.-I. *Nature* **1989**, *342*, 248.

14. Holmgren, A.; Kuehn, M. J.; Brändén, C.-I.; Hultgren, S. J. *EMBO J*. **1992**, *11*, 1617.

15. Kuehn, M. J.; Ogg, D. J.; Kihlberg, J.; Slonim, L. N.; Flemmer, K.; Bergfors, T.; Hultgren, S. J. *Science* **1993**, *262*, 1234.

16. Xu, Z.; Jones, C. H.; Haslam, D.; Pinkner, J. S.; Dodson, K.; Kihlberg, J.; Hultgren, S. J. *Mol. Microbiol*. **1995**, *16*, 1011.

17. Stephens, C.; Shapiro, L. *Chem. Biol*. **1997**, *4*, 637.

18. Flemmer Karlsson, K.; Walse, B.; Drakenberg, T.; Kihlberg, J. *Lett. Peptide Sci*. **1996**, *3*, 143.

19. Cameron, L. R.; Holder, J. L.; Meldal, M.; Sheppard, R. C. *J. Chem. Soc. Perkin Trans. 1*. **1988**, 2895.

20. Garegg, P. J.; Samuelsson, B. *J. Chem. Soc. Perkin Trans. 1*. **1980**, 2866.

21. Carpino, L. A.; El-Faham, A.; Minor, C. A.; Albericio, F. *J. Chem. Soc., Chem. Commun*. **1994**, 201.

22. Carpino, L. A. *J. Am. Chem. Soc*. **1993**, *115*, 4397.

23. Carpino, L. A.; El-Faham, A. *J. Org. Chem*. **1994**, *59*, 695.

24. Flemmer, K.; Xu, Z.; Pinkner, J. S.; Hultgren, S. J.; Kihlberg, J. *Bioorg. Med. Chem. Lett*. **1995**, *5*, 927.

25. Derrick, J. P.; Wigley, D. B. *Nature* **1992**, *359*, 752.

26. Wüthrich, K. *NMR of Proteins and Nucleic Acids*; New York: Wiley & Sons, 1986.

27. Dyson, H. J.; Wright, P. E. *Annu. Rev. Biophys. Biophys. Chem*. **1991**, *20*, 519.

28. Bundi, A.; Grathwohl, C.; Hochmann, J.; Keller, R. M.; Wagner, G.; Wüthrich, K. *J. Magn. Reson*. **1975**, *18*, 191.

29. Wishart, D. S.; Bigham, C. G.; Holm, A.; Hodges, R. S.; Sykes, B. D. *J. Biomol. NMR*. **1995**, *5*, 67.

30. Gronenborn, A. M.; Clore, G. M. *Crit. Rev. Biochem. Mol. Biol*. **1995**, *30*, 351.

31. Ni, F. *Prog. Nucl. Magn. Reson. Spectrosc*. **1994**, *26*, 517.

32. The off-rate for dissociation of the heptapeptide PapG308-314 from the complex with PapD was estimated in the following way. The rate of peptide association with PapD was assumed to be diffusion limited ($10^8\,M^{-1}\,s^{-1}$). A dissociation constant of $\sim 10^{-6}$ M has been determined for a modified PapG307-314 peptide (G. Soto, personal communication), resulting in an off-rate of $\sim 100\,s^{-1}$ for this octapeptide. Since PapG308-314 is a weaker inhibitor than the octapeptide PapG307-314, the off-rate of PapG308-314 should be even higher, thus corresponding to the fast exchange regime.

33. Neuhaus, D.; Williamson, M. P. *The nuclear Overhauser effect in structural and conformational analysis*; New York: VCH Publishers, 1989.

34. Walse, B.; Kihlberg, J.; Flemmer Karlsson, K.; Nilsson, M.; Wahlund, K.-G.; Pinkner, J. S.; Hultgren, S. J.; Drakenberg, T. *FEBS Lett*. **1997**, *412*, 115.

35. Campbell, A. P.; Sykes, B. D. *Annu. Rev. Biophys. Chem. Biomol. Struct*. **1993**, *22*, 99.

36. Kuboniwa, H.; Grzesiek, S.; Delaglio, F.; Bax, A. *J. Biomol. NMR*. **1994**, *4*, 871.

37. Smith, L. J.; Bolin, K. A.; Schwalbe, H.; MacArthur, M. W.; Thornton, J. M.; Dobson, C. M. *J. Mol. Biol*. **1996**, *255*, 494.

38. The differences in chemical shift observed for some of the residues in PapG308-314 on addition of PapD may appear to be small (0.01 ppm). However, the observed chemical shift is an

average of the shift for free and bound peptide. Since a peptide:PapD ratio of 25:1 was used in the NMR studies the ratio between free and bound peptide is >25:1. Thus, the actual chemical shift difference between the free and bound form could be estimated to be ~0.3 ppm, or even greater.

39. Gallop, M. A.; Barrett, R. W.; Dower, W. J.; Fodor, S. P. A.; Gordon, E. M. *J. Med. Chem.* **1994**, *37*, 1233.

40. Gordon, E. M.; Barrett, R. W.; Dower, W. J.; Fodor, S. P. A.; Gallop, M. A. *J. Med. Chem.* **1994**, *37*, 1385.

41. Thompson, L. A.; Ellman, J. A. *Chem. Rev.* **1996**, *96*, 555.

42. Fersht, A. R.; Shi, J. P.; Knill-Jones, J.; Lowe, D. M.; Wilkinson, A. J.; Blow, D. M.; Brick, P.; Carter, P.; Waye, M. M. Y.; Winter, G. *Nature* **1985**, *314*, 235.

43. Barlos, K.; Chatzi, O.; Gatos, D.; Stavropoulos, G. *Int. J. Peptide Protein Res.* **1991**, *37*, 513.

44. Rink, H. *Tetrahedron Lett.* **1987**, *28*, 3787.

45. Bernatowicz, M. S.; Daniels, S. B.; Köster, H. *Tetrahedron Lett.* **1989**, *30*, 4645.

46. Aue, W. P.; Bartholdi, E.; Ernst, R. R. *J. Chem. Phys.* **1976**, *64*, 2229.

47. Rance, M.; Sorensen, O. W.; Bodenhausen, G.; Wagner, G.; Ernst, R. R.; Wüthrich, K. *Biochem. Biophys. Res. Commun.* **1983**, *117*, 479.

48. Braunschweiler, L.; Ernst, R. R. *J. Magn. Reson.* **1983**, *53*, 521.

49. Bax, A.; Davis, D. G. *J. Magn. Reson.* **1985**, *65*, 355.

50. Davis, D. G.; Bax, A. *J. Am. Chem. Soc.* **1985**, *107*, 2820.

51. Jeener, J.; Meier, B. H.; Bachmann, P.; Ernst, R. R. *J. Chem. Phys.* **1979**, *71*, 4546.

52. Kumar, A.; Ernst, R. R.; Wüthrich, K. *Biochem. Biophys. Res. Comm.* **1980**, *95*, 1.

53. Macura, S.; Ernst, R. R. *Mol. Phys.* **1980**, *41*, 95.

54. Bothner-By, A. A.; Stephens, R. L.; Lee, J.-M.; Warren, C. D.; Jeanloz, R. W. *J. Am. Chem. Soc.* **1984**, *106*, 811.

55. Bax, A.; Davis, D. G. *J. Magn. Reson.* **1985**, *63*, 207.

56. Rance, M. *J. Magn. Reson.* **1987**, *74*, 557.

57. Shaka, A. J.; Lee, C. J.; Pines, A. *J. Magn. Reson.* **1988**, *77*, 274.

58. States, D. J.; Haberkorn, R. A.; Ruben, D. J. *J. Magn. Reson.* **1982**, *48*, 286.

59. Leathers, V. L.; Linse, S.; Forsén, S.; Norman, A. W. *J. Biol. Chem.* **1990**, *265*, 9838.

60. Piotto, M.; Saudek, V.; Sklenár, V. *J. Biomol. NMR.* **1992**, 661.

61. Hwang, T.-L.; Shaka, A. J. *J. Magn. Reson. A.* **1995**, *112*, 275.

62. Zhang, O.; Kay, L. E.; Olivier, J. P.; Forman-Kay, J. D. *J. Biomol. NMR.* **1994**, *4*, 845.

63. Cavanagh, J.; Rance, M. *J. Magn. Reson.* **1992**, *96*, 670.